

# Low-Velocity Impact of Nanocomposite and Polymer Plates

Jeremy Gustin, Brian Freeman, James Stone, Mohammad Mahinfalah, Amin Salehi-Khojin

Department of Mechanical Engineering and Applied Mechanics, North Dakota State University, Fargo, North Dakota 58105

Received 4 May 2004; accepted 30 September 2004

DOI 10.1002/app.21433

Published online in Wiley InterScience (www.interscience.wiley.com).

**ABSTRACT:** Nanocomposites are more widely studied today because of higher stiffness, decreased permeability, thermal stability, and many other properties superior to those of regular polymers. However, manufacturers are concerned about implementing nanocomposites because of their lower impact properties with respect to the base polymer. This study focused on low-velocity impact tests of a thermoplastic olefin by itself and with 5 wt % nanoclay. The impact tests were conducted at  $-40$ ,  $23.9$ , and  $65.6^{\circ}\text{C}$  until

the polymer and nanocomposite plates experienced complete striker penetration. The force–time and force–deflection responses obtained from the impact testing provided a means of comparing the impact performances of the two materials. © 2005 Wiley Periodicals, Inc. *J Appl Polym Sci* 96: 2309–2315, 2005

**Key words:** nanocomposites; impact resistance; stiffness

## INTRODUCTION

Polymer nanocomposites constitute a new class of materials. They are hybrid structures consisting of an organic phase (polymer) and an inorganic phase (layered silicate).<sup>1</sup> The combination of the organic and inorganic phases results in the beneficial properties of both materials, which can include low density, flexibility, good moldability, high strength, heat stability, and chemical resistance.<sup>2</sup> For the first time, there is an opportunity to design materials without the compromises typically found in conventionally filled polymer composites.<sup>3</sup> Uses for this new class of materials can be found in aerospace, automotive, electronic, and biotechnology applications. There is clear evidence that nanocomposites offer significant performance improvements over their base polymers. According to the material combination, most of the static properties can be improved. Perhaps the most interesting benefits are to the elastic modulus and the compression strength. However, the increased stiffness typically results in lower impact performance. Clearly, this is an issue requiring consideration for applications for which impact loading events are likely.<sup>4</sup>

This article presents the effects of temperature on the impact properties of a thermoplastic olefin by itself and with 5 wt % nanoclay added to its polymer matrix. The nanoclay additive, Cloisite 15A, was pro-

duced by Southern Clay Products, Inc. In this study, the impact properties of the polymer and nanocomposite were compared at  $-40^{\circ}\text{C}$ ,  $23.9^{\circ}\text{C}$ , and  $65.6^{\circ}\text{C}$ . Impact tests were performed at each temperature, with impact energies increasing from 7 J until failure of the material.

## BACKGROUND

The layered silicates used in the nanocomposites had a layer thickness of about 1 nm, with the lateral dimensions varying between 20 nm and tens of micrometers, depending on the source of the clay. Figure 1 shows a high-resolution transmission electron micrograph of a single silicate in polyamide 12.

Three polymer-layered silicate morphologies can be achieved, as shown in Figure 2. The first is phase-separated and occurs when the nanoclay is not separated from itself and is in large aggregate clumps inside the polymer matrix.<sup>5</sup> This happens when the polymer is unable to intercalate between the silicate sheets. When the silicate is in this form, it has no or little effect on the properties of the polymer. The second morphology is intercalated; this is when a single extended polymer chain is intercalated between the silicate layers, and this results in a well-ordered multilayer morphology built up with alternating polymeric and inorganic layers. The third morphology is when the silicate layers are completely and uniformly dispersed in a continuous polymer matrix. This is known as an exfoliated or delaminated structure. For this study, Cloisite 15A was exfoliated in the polyolefin.

Correspondence to: J. Gustin (jeremy.gustin@ndsu.nodak.edu).



**Figure 1** High-resolution transmission electron micrograph showing single platelet layers.<sup>1</sup>

Cloisite 15A is a natural montmorillonite modified with a quaternary ammonium salt. Montmorillonite is a type of smectite clay mineral that tends to swell when exposed to water. Montmorillonite forms through the alteration of silicate minerals under alkaline conditions in basic igneous rocks, such as volcanic ash, which can accumulate in the oceans.<sup>6</sup> Cloisite 15A nanoclays are high-aspect-ratio additives based on montmorillonite clay and designed and manufactured by Southern Clay Products, Inc.<sup>6</sup> The chemical structure of Cloisite 15A is shown in Figure 3. The loose and packed bulk densities, along with the specific weights of Cloisite 15A, are given in Table I.

Nanofillers have been proved to trigger mechanical property improvements of the polymers in which they are dispersed. As an example, Lan<sup>7</sup> reported that nylon 6 reinforced with 4.7 wt % montmorillonite clay achieved many improved properties in comparison with the nylon-6 polymer itself. The 4.7 wt % montmorillonite clay nanocomposite had a tensile strength of 97.2 MPa, a tensile modulus of 1.87 GPa, and a heat-distortion temperature of 152°C; these were 68.6

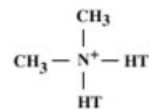


**Figure 3** Cloisite 15A chemical structure (HT = hydrogenated tallow).<sup>6</sup>

MPa, 1.11 GPa, and 65°C, respectively, for the nylon-6 polymer.

Most studies of nanocomposites focus on improvements in the mechanical strength and moduli, heat-deflection temperature barrier properties, flame retardancy, and oxygen resistance.<sup>8-17</sup> However, few have done studies on the impact strength of nanocomposites. One of the tradeoffs of using nanocomposites instead of a standard polymer is that the impact failure of nanocomposites is generally more brittle; for certain situations, this could be a detriment.

Bureau<sup>17</sup> studied the mechanical behavior of compression-molded polyamide 6 (PA6) reinforced with 2 wt % organonanoclay (montmorillonite intercalated with  $\omega$ -amino dodecanoic along with PA6). The tensile strength and Young's modulus of the PA6 nanocomposite were 15% higher than those for PA6 alone.

McNally et al.<sup>1</sup> determined the mechanical and impact properties of polyamide 12/quaternary tallow ammonium chloride modified with a fluoromica nanocomposite (PA12-MAE), polyamide 12/tetrasilicic fluoromica (PA12-ME100), and PA12 alone. The results are listed in Table II, which allows a comparison of PA12-MAE and PA12-ME100 nanocomposites with PA12.

The effect of nanoclay on the impact properties of polycarbonate (PC) nanocomposites was studied by Hsieh.<sup>18</sup> Hsieh showed that the amount of nanoclay added was critical to the ballistic performance. Nanocomposites with 5 wt % or more showed brittle failure when impacted, whereas nanocomposites with less than 5 wt % showed a ductile mode of failure. However, 2.5 wt % led to decreased ductility in comparison with that of standard PC. As the weight percentage of nanoclay increased, the ductility of the polymer decreased, and this resulted in lower absorbed energies during impact. This loss of ductility has to be researched when a nanoclay is added to different polymers.

## EXPERIMENTAL

The testing materials were 95.25-mm<sup>2</sup> samples 3.175 mm thick that were made of TPO and TPO with 5 wt % 15A

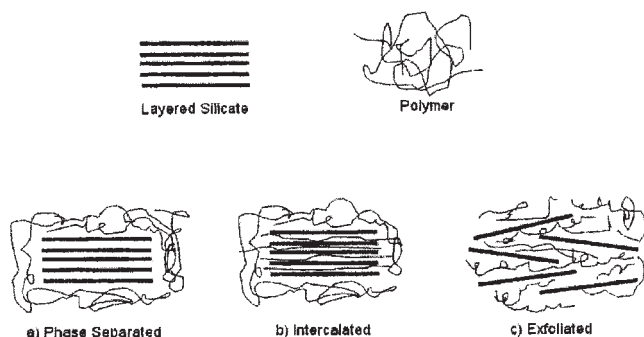


**Figure 2** Different types of composites arising from the interaction of layered silicates and polymers: (a) phase-separated microcomposite, (b) intercalated nanocomposite, and (c) exfoliated nanocomposite.

**TABLE I**  
Densities of Cloisite 15A<sup>6</sup>

Loose bulk (kg/m <sup>3</sup> )	Packed bulk (kg/m <sup>3</sup> )	Specific gravity
172.8	298.6	1.66

**TABLE II**  
Mechanical and Impact Data for PA12, PA12-ME100, and PA12-MAE<sup>1</sup>

Property	PA12	PA12-ME100	PA12-MAE
Tensile strength (MPa)	32.2	32.0	48.2
Tensile modulus (MPa)	177	197	224
Flexural strength (MPa)	11.2	11.5	12.5
Flexural modulus (MPa)	378	459	570
Impact strength at 23°C (kJ)	14.5	14	13.4
Impact strength at -40°C (kJ)	17.7	8.3	1.7

**TABLE III**  
Maximum Force Data

Sample type	Impact temperature (°C)	Maximum force (kN)
Nanocomposite	-40	3.5
Nanocomposite	23.9	1.7
Nanocomposite	65.6	1.1
Polymer	-40	3.25
Polymer	23.9	1.7
Polymer	65.6	1.1

nanoclay from Southern Clay Products, Inc. An Instron Dynatup 9250HV drop tower was used for impact testing. This machine was capable of impacting samples at energies of up to 826 J with a spring assist. For this study, all samples were impacted with a 7.25-kg drop weight. A pneumatic clamping fixture, with a 76.2-mm (3-in.)-diameter opening, secured each sample during impact. The samples were impacted with a 12.7-mm (0.5-in.)-diameter hemispherical tip striker, which was constructed out of high-strength steel. Impulse software was used to display and record the impact data. The Impulse software recorded the absorbed energy by calculating the change in the kinetic and potential energy beginning at sample impact. An environmental chamber was used to control the impact temperatures. The samples were placed inside the environmental chamber for a minimum of 10 min before impact to ensure temperature equilibrium.

**RESULTS**

**Absorbed impact energy**

The impact performance of the nanocomposite and polymer were characterized by a consideration of the maxi-

imum absorbed energy. Figure 4 shows that the temperature had a significant effect on the impact performance of the two materials. As the temperature decreased from 65.6 to -40°C, the maximum absorbed energy for both materials increased substantially. The maximum absorbed energy of the nanocomposite increased from 19.75 (65.6°C) to 31.5 (23.9°C) and 37 J (-40°C). The maximum absorbed energy of the polymer increased from 19.75 (65.6°C) to 29.3 (23.9°C) and 52 J (-40°C).

The impact performance of the two materials at each impact temperature is shown in Figure 4. At 65.6°C, no significant difference occurred between the two materials, with both having maximum absorbed energies around 19.75 J. The two materials also had a similar impact performance at 23.9°C, with the maximum absorbed energies of the nanocomposite and polymer being 31.5 and 29.3 J, respectively. A significant difference occurred in the impact performance of the two materials at -40°C. At this temperature, the maximum absorbed energies of the nanocomposite and polymer were 37 and 52 J, respectively. This corresponded to a 29% lower maximum absorbed energy for the nanocomposite compared with that of the polymer. In addition, at the impact energy of 42 J (-40°C), all three nanocomposite samples shattered. For this

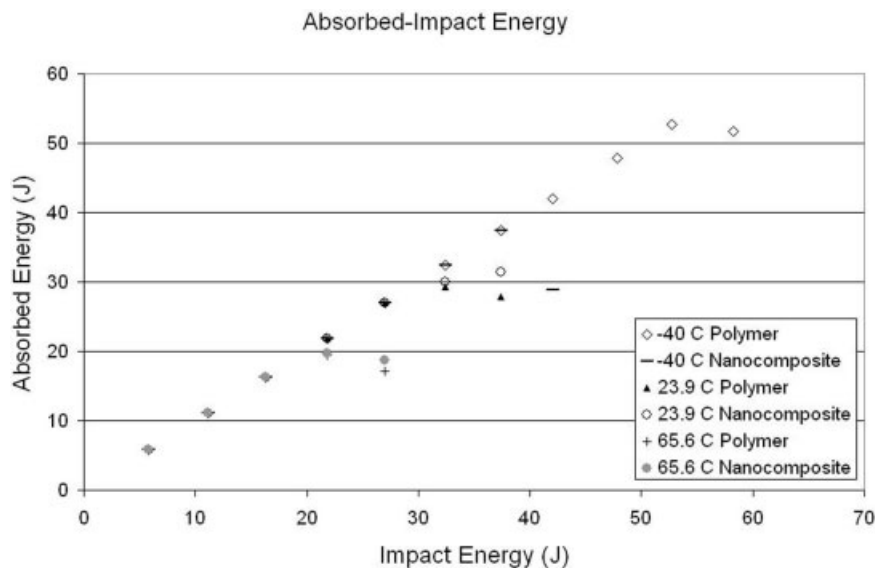


**Figure 4** Absorbed energy versus the impact energy for the nanocomposite and polymer.

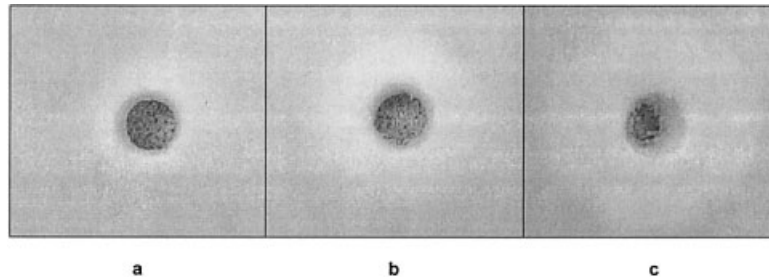


**Figure 5** Front damage area of the polymer: (a) 22 J and 65.6°C, (b) 37 J and 23.9°C, and (c) 42 J and  $-40^{\circ}\text{C}$ .

same impact, the striker completely penetrated the three polymer samples, but none shattered.

### Force and time

The nanocomposite and polymer force–time graphs for the three different impact temperatures are in the appendix. Each graph illustrates how different impact energies affected the force response. In general, higher forces were reached as the impact energy was increased. Table III lists the maximum forces at the three different impact temperatures. The comparison of these results illustrates the considerable effect that the impact temperature had on the maximum force, which likely resulted from increased flexural stiffness.

### Impact damage

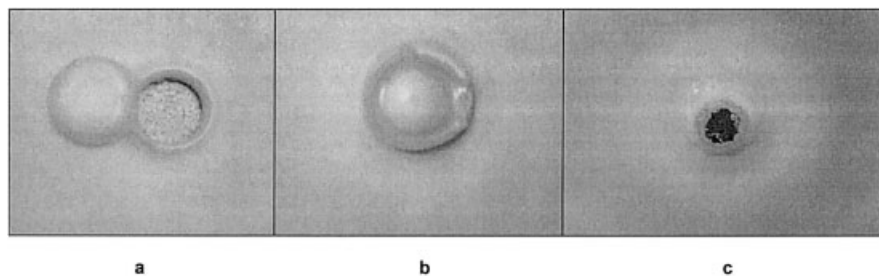
The damage area of the samples is shown in Figures 5–8. The impact energies correspond to the impact

energy that resulted in failure of the nanocomposite. A shattered nanocomposite, impacted at 42 J and  $-40^{\circ}\text{C}$ , is shown in Figure 7. This shows that  $-40^{\circ}\text{C}$  was below the glass-transition temperature of the nanocomposite.

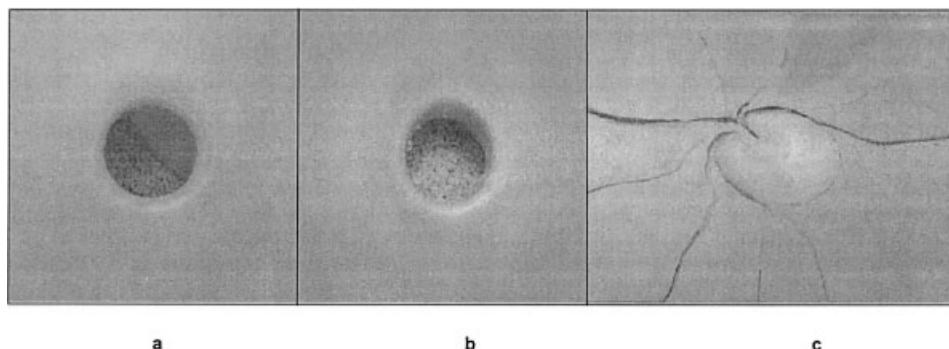
### Force and deflection

Figure 9(a,b) presents force–deflection curves for the nanocomposite and polymer plates at the three impact temperatures. The dynamic stiffness corresponds to the slope of the curves. As the temperature increased, the dynamic stiffness of the samples decreased substantially. This likely occurred as a result of thermal expansion, which caused the molecules to move farther apart.

Figure 9(b) shows the force–deflection curve for the polymer at all three temperatures. As the temperature decreased, the dynamic stiffness of the samples increased; this was very similar to that of the nanocom-



**Figure 6** Back damage area of the polymer: (a) 22 J and 65.6°C, (b) 37 J and 23.9°C, and (c) 42 J and  $-40^{\circ}\text{C}$ .



**Figure 7** Front damage area of the nanocomposite: (a) 22 J and 65.6°C, (b) 37 J and 23.9°C, and (c) 42 J and  $-40^{\circ}\text{C}$ .



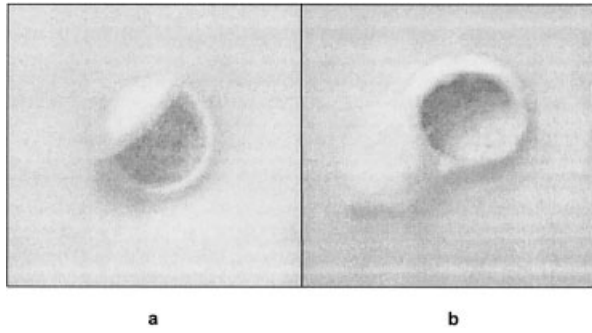


**Figure 8** Back damage area of the nanocomposite: (a) 22 J and 65.6°C and (b) 37 J and 23.9°C.

posite. The slight increase in the dynamic stiffness of the nanocomposite over the polymer can possibly be attributed to the creation of a three-dimensional network of interconnected silicate layers, which strengthened the material through mechanical percolation and the presence of hydrogen bonds assumed to take place between silica particles instead of Van der Waals bonding.

**CONCLUSIONS**

Low-velocity impact tests were conducted on nanocomposite and polymer plates at three temperatures

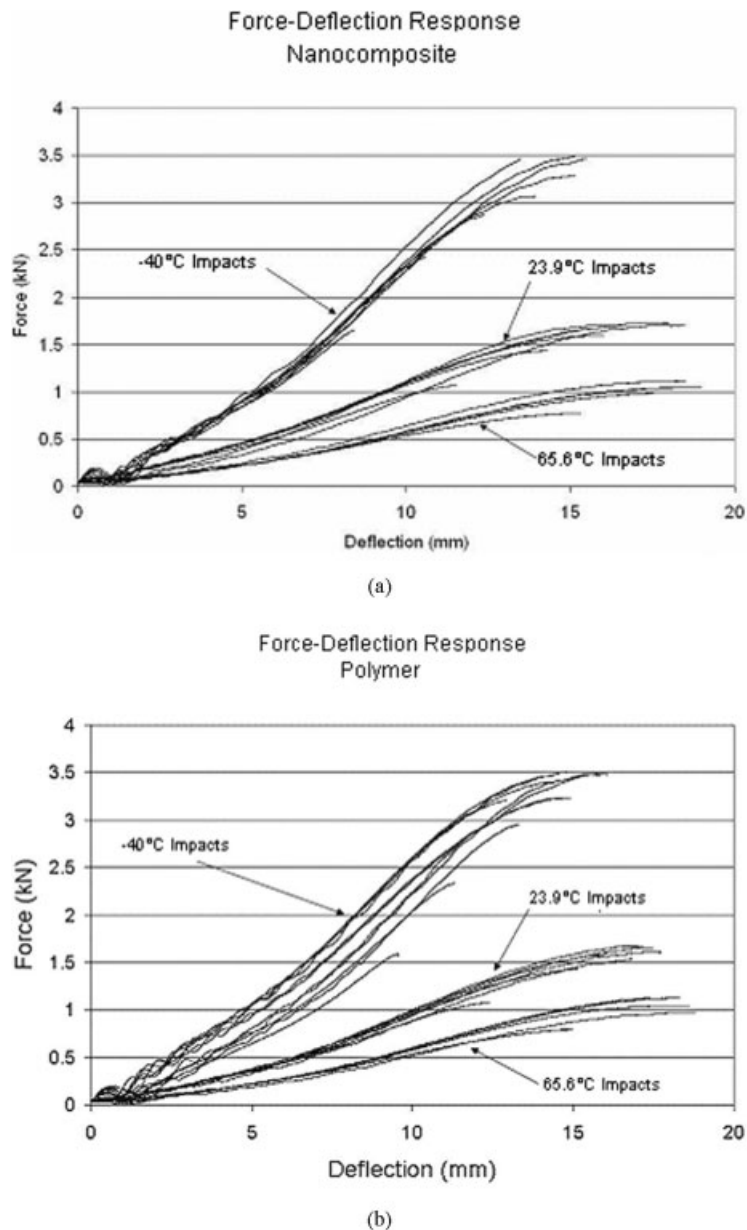


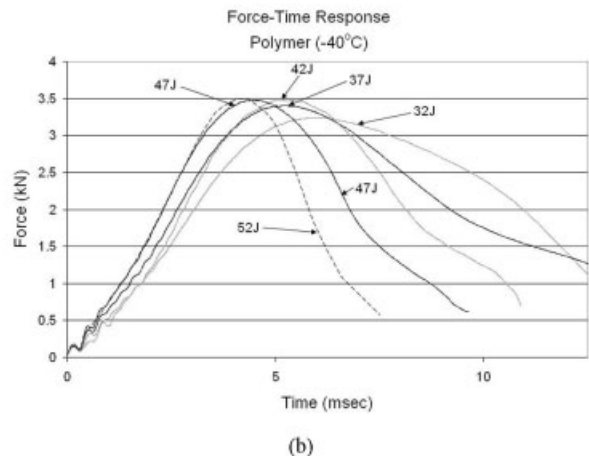
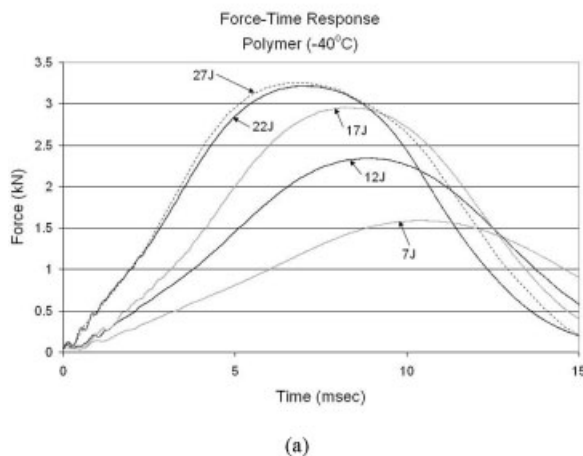
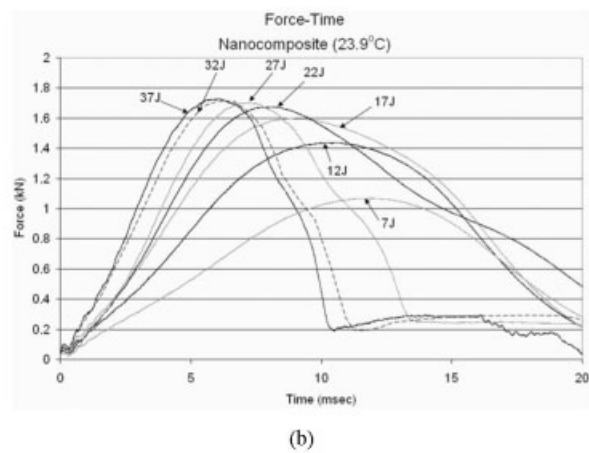
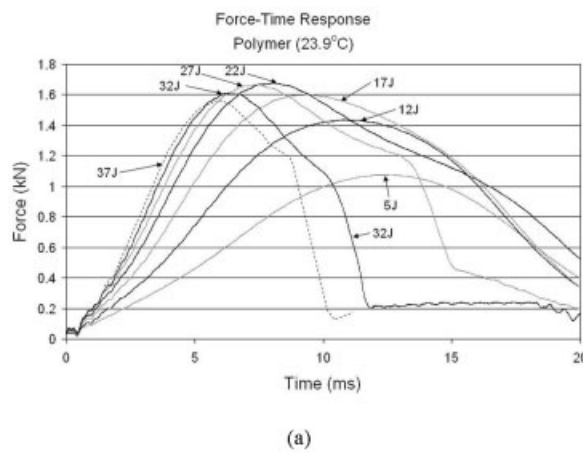
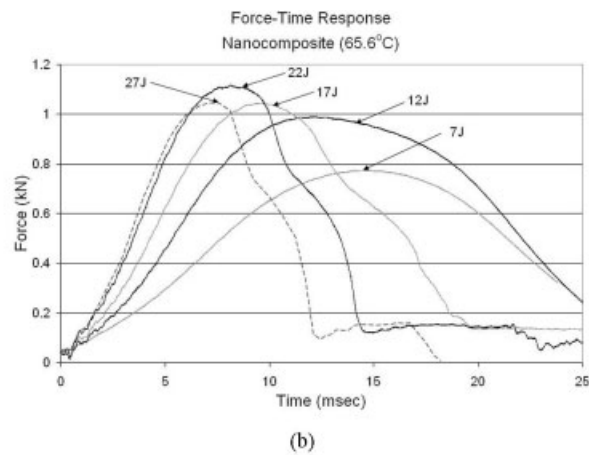
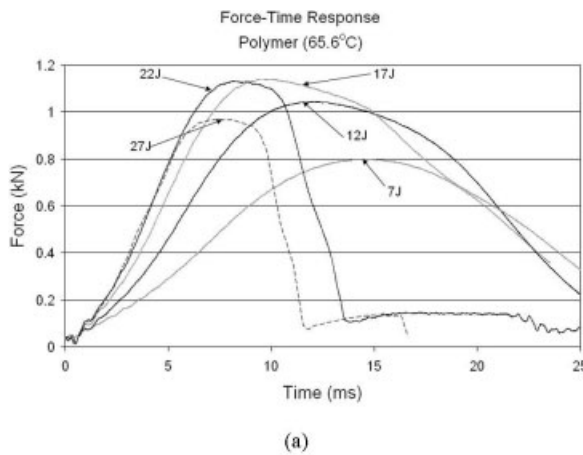
**Figure 9** Force versus the deflection for (a) the nanocomposite and (b) the polymer.

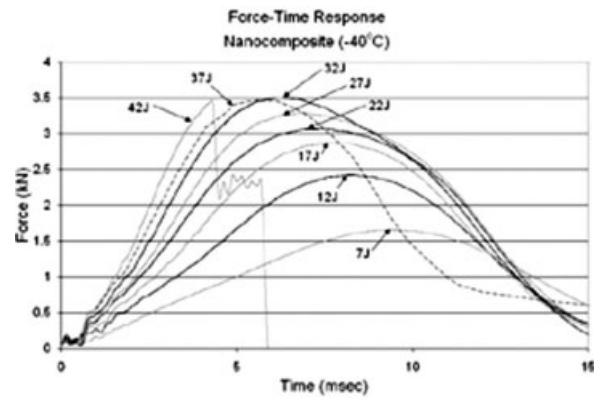
(-40, 23.9, and 65.6°C) until complete striker penetration occurred. The impact results illustrated how the impact performance of the polymer and nanocomposite were similar at 23.9 and 65.6°C but varied at -40°C. At -40°C, the maximum absorbed energy of the nanocomposite was 29% lower than that of the polymer. In addition, at -40°C, the polymer experienced only local damage at 57 J, whereas the nanocomposite shattered at the 42-J impact. Recommendations for improving the impact performance include

changing the clay content and possibly further improving the clay dispersion throughout the polymer. Additional research could include impact testing at additional temperatures, which would provide information on the glass-transition temperatures of both materials.

The authors thank Doug Hunter at Southern Clay Products, Inc., for the donation of the thermoplastic olefin and nanocomposite.

APPENDIX





(c)

## References

1. McNally, T.; Murphy, W.; Lew, C.; Turner, R.; Brennan, G. *Polymer* 2003, 44, 2761.
2. Chang, H.; Kim, S.; Joo, Y.; Im, S. *Polymer* 2004, 45, 919.
3. Schmidt, D.; Shah, D.; Giannelis, E. *Curr Opin Solid State Mater Sci* 2002, 6, 205.
4. Okamoto, M. *Rapa Rev Rep* 2003, 14, 163.
5. Schlumberger Oilfield Services. <http://www.slb.com> (accessed March 2004).
6. Southern Clay Products, Inc. <http://www.nanoclay.com> (accessed March 2004).
7. Lan, T. *Chem Mater* 1994, 6, 573.
8. Ogata, N. *J Appl Polym Sci* 1997, 66, 573.
9. Reichert, P.; Nitz, H. *Mater Eng* 2000, 8, 275.
10. Ma, J.; Hu, Y. *J Appl Polym Sci* 2001, 82, 3611.
11. Zanetti, M.; Camino, G.; Reichert, P.; Mülhaupt, R. *Macromol Rapid Commun* 2001, 22, 176.
12. Zanetti, M.; Camino, G. *Chem Mater* 2002, 14, 189.
13. Gilman, J.; Jackson, C. *Chem Mater* 2000, 12, 1866.
14. Messersmith, P. *J Polym Sci Part A: Polym Chem* 1995, 33, 1047.
15. Murase, S.; Inoue, A. *J Polym Sci Part B: Polym Phys* 2002, 40, 479.
16. LeBaron, P. C. *Appl Clay Sci* 1999, 15, 11.
17. Bureau, M. *Polym Eng Sci* 2002, 42, 1897.
18. Hsieh, A. *Annu Tech Conf* 2001, 2, pp 6-433.